THE JOURNAL OF BIOLOGICAL CHEMISTRY VOL. 287, NO. 30, pp. 25060–25072, July 20, 2012

Intra- and Interprotein Phosphorylation between Two-hybrid Histidine Kinases Controls *Myxococcus xanthus* Developmental Progression*[S]

Received for publication, June 1, 2012 Published, JBC Papers in Press, June 1, 2012, DOI 10.1074/jbc.M112.387241

Andreas Schramm[1], **Bongsoo Lee**[2], **and Penelope I. Higgs**[3]

From the Department of Ecophysiology, Max Planck Institute for Terrestrial Microbiology, 35043 Marburg, Germany

Background: His-Asp phosphorelay proteins can be components of complex signaling systems.
Results: Two hybrid histidine kinases, EspA and EspC, form a signaling complex; EspA phosphorylates both receiver modules to regulate proteolytic turnover of a regulatory protein.
Conclusion: Two hybrid histidine kinases are integrated by inter- and intra-histidine aspartate phosphotransfer.
Significance: A novel His-Asp phosphorelay signal transduction mechanism was identified.

Histidine-aspartate phosphorelay signaling systems are used to couple stimuli to cellular responses. A hallmark feature is the highly modular signal transmission modules that can form both simple "two-component" systems and sophisticated multicomponent systems that integrate stimuli over time and space to generate coordinated and fine-tuned responses. The deltaproteobacterium *Myxococcus xanthus* contains a large repertoire of signaling proteins, many of which regulate its multicellular developmental program. Here, we assign an orphan hybrid histidine protein kinase, EspC, to the Esp signaling system that negatively regulates progression through the *M. xanthus* developmental program. The Esp signal system consists of the hybrid histidine protein kinase, EspA, two serine/threonine protein kinases, and a putative transport protein. We demonstrate that EspC is an essential component of this system because Δ*espA*, Δ*espC*, and Δ*espA* Δ*espC* double mutants share an identical developmental phenotype. Neither substitution of the phosphoaccepting histidine residue nor deletion of the entire catalytic ATPase domain in EspC produces an *in vivo* mutant developmental phenotype. In contrast, substitution of the receiver phosphoaccepting residue yields the null phenotype. Although the EspC histidine kinase can efficiently autophosphorylate *in vitro*, it does not act as a phosphodonor to its own receiver domain. Our *in vitro* and *in vivo* analyses suggest the phosphodonor is instead the EspA histidine kinase. We propose EspA and EspC participate in a novel hybrid histidine protein kinase signaling mechanism involving both inter- and intraprotein phosphotransfer. The output of this signaling system appears to be the combined phosphorylated state of the EspA and EspC receiver modules. This system regulates the proteolytic turnover of MrpC, an important regulator of the developmental program.

Signal transmission via reversible histidine-aspartate (His-Asp) phosphorelay (often termed two-component signal transduction) is a widely used mechanism for coupling specific stimuli to appropriate cellular responses (1). Genes encoding these proteins can be identified in nearly all bacteria, certain eukaryotic microorganisms, plants, and archaea (2). Members of this signal transduction family can be identified by the presence of highly conserved histidine kinase (HK)[4] or receiver (REC) signal transmission modules. The HK module consists of a dimerization/histidine phosphotransfer (DHp, also known as HisKA) domain and a catalytic ATP hydrolysis (CA, also known as HATPase_c) domain (3). HK modules are dimeric and interact through the DHp domain; autophosphorylation (HK∼P) occurs by CA-dependent transfer of the γ-phosphoryl group of ATP to an invariant histidine residue in the DHp domain (4). The single "switch" domain REC module catalyzes transfer of a phosphoryl group from an HK∼P, or sometimes from a small molecule phosphodonor, onto an invariant aspartate residue within itself (5, 6). REC phosphorylation is thought to shift the equilibrium between inactive and active conformations. Most HK modules also display phosphatase activity toward the cognate REC∼P, and a phosphatase motif (E/D)*XX*(N/T) has been identified adjacent to the phosphoaccepting His residue in the DHp domain (7). The CA domain also modulates phosphatase activity (8, 9).

In the paradigm two-component system, the HK and REC modules are organized into two separate proteins as follows: a sensor histidine protein kinase (HPK) containing an N-terminal stimulus-sensing domain that modulates activity of the associated HK module, and a response regulator protein (RR) in

* This work was supported in part by the Max Planck Society.
[S] This article contains supplemental Fig. S1, Tables S1 and S2, and Methods.
[1] Supported by the International Max Planck Research School for Environmental, Cellular, and Molecular Microbiology.
[2] Present address: Dept. of Agricultural Biotechnology, Seoul National University, Seoul 151-921, South Korea.
[3] To whom correspondence should be addressed: Dept. of Ecophysiology, Max Planck Institute for Terrestrial Microbiology, Karl-von-Frisch-Strasse 10, 35043, Marburg, Germany. Tel.: 49-6421-178301; Fax: 49-6421-178309; E-mail: higgs@mpi-marburg.mpg.de.

[4] The abbreviations used are: HK, histidine kinase region; HPK, histidine protein kinase; HyHPK, hybrid histidine protein kinase; REC, receiver; RR, response regulator; DHp, dimerization and histidine phosphotransfer domain; CA, catalytic ATPase; FHA, forkhead associated domain, PAS, Per Arnt Sim sensing domain; MASE1, membrane-associated sensing domain 1; IB, inclusion body; aa, amino acid; LSB, Laemmli sample buffer.

which the N-terminal REC domain modulates the activity of an associated effector domain. HPK stimulus-sensing domains are highly variable (10), whereas RR effector domains are most often promoter-binding elements but also include enzymatic or protein-interaction output domains (11). Finally, some RRs, termed "stand alone" receivers lack an associated output domain and mediate signal output by directly interacting with target proteins.

A variation of the simple two-component signal pathway involves hybrid histidine protein kinases (HyHPK) in which one (or sometimes more) REC domain is fused to the HK at the C terminus. Typically, HyHPKs participate in a four-step phosphorelay in which the phosphoryl group is passed from the HyHPK to a histidine phosphotransferase protein and then to an output-mediating RR (12). Multistep phosphorelay systems are proposed to provide additional regulatory sites for fine-tuning signal output. HyHPKs can also function in the absence of histidine phosphotransferase proteins. In these cases, the fused REC domain(s) have been shown to modulate signal transmission to a cognate RR by functioning to inactivate the associated kinase (13) and/or to provide sites for alternative kinase phosphorylation presumably leading to signal integration (14). Thus, HyHPKs provide an excellent example of how the highly modular nature of His-Asp phosphorelays can be exploited to generate complex signaling systems.

HyHPKs represent only 20% of the HKs in bacteria but 90% of the HKs in eukaryotes (2, 15). In general, these more complex signaling systems are favored in organisms that regulate complex behaviors. Perhaps the best example can be observed among the Myxobacteria, a group within the Deltaproteobacteria, which favor a "social" (multicellular) life cycle. Several of the developing myxobacterial species (16–19) encode a large repertoire of signal transduction genes (20–24). *Myxococcus xanthus*, the best studied of the Myxobacteria, contains 272 His-Asp phosphorelay family homologs (24). Only 29% of the 251 (nonchemosensory related) His-Asp phosphorelay genes are encoded together as HPK-RR pairs (*i.e.* two-component systems); instead, 58% are genetically orphan, and the remaining 16% encoded in complex gene clusters (24) are indicative of nonlinear complex signaling pathways (9). One of the challenges in analysis of *M. xanthus* signaling pathways is to assign orphan His-Asp phosphorelay proteins to signaling pathways and to define the wiring networks.

That *M. xanthus* requires sophisticated signaling systems is perhaps no surprise given its complex life cycle. Under nutrient-limited conditions, the cells enter a complex developmental pathway involving at least three distinct cell fates. Some cells are induced to aggregate into mounds containing $\sim 10^5$ cells and, exclusively inside these mounds, are triggered to differentiate into quiescent, environmentally resistant spores (25). Other cells instead lyse during development apparently via programmed cell death (26–28). Finally, a minor proportion of the developing population differentiate into a persister-like state termed peripheral rods (29, 30). Formation of fruiting bodies (31–34), sporulation (34, 35), and possibly programmed cell death (28) are regulated by MrpC, a transcriptional regulator that is up-regulated during development and is subject to both negative (33, 36) and positive (31, 34) regulation.

Progression through the developmental program is negatively regulated by several atypical His-Asp phosphorelay proteins (9, 37–39). The Esp (early sporulation) signaling system is an unusually complex multicomponent system consisting of two serine/threonine kinases (PktA5 and PktB8), a putative oligopeptide transport protein (EspB), and a HyHPK (EspA). Based on genetic and biochemical analyses, EspA autophosphorylates and donates a phosphoryl group to its associated receiver to delay developmental progression by preventing accumulation of MrpC (36). It is thought that the delay of development is released by modulation of EspA activity via the upstream signaling module consisting of EspB, PktA5, and PktB8 (40, 41). However, both the exact output and the signals modulating this system are unknown.

In this study, we demonstrate that EspC, a genetic orphan HyHPK, is an essential component of the Esp signaling system. Using a combination of genetic and *in vitro* biochemical approaches, we demonstrate that EspA and EspC function in a novel HyHPK mechanism involving inter- and intra-HyHPK phosphotransfer. The target of this sophisticated signaling system is the regulated proteolysis of a crucial developmental regulatory protein, MrpC. This signaling system provides an important example of the inherent adaptability and plasticity of the histidine-aspartic acid phosphorelay proteins.

EXPERIMENTAL PROCEDURES

Bacterial Strains and Growth Conditions—Bacterial strains and plasmids used in this study are listed in Table 1. *M. xanthus* strains were grown under vegetative conditions on casitone yeast extract medium broth or agar plates as described previously (36, 42). Plates were supplemented with 100 μg ml^{-1} kanamycin, where necessary. *Escherichia coli* cells were grown under standard laboratory conditions in lysogeny broth media (43) supplemented with 50 μg ml^{-1} kanamycin where necessary. *M. xanthus* development was induced under submerged culture conditions in either a 16- or 0.5-ml format, as described previously (36, 42). Briefly, exponentially growing cells were diluted to an optical density of 0.035 A_{550} in casitone yeast extract medium. 16 or 0.5 ml of the diluted culture was seeded in 85-mm Petri dishes or 24-well plates (Sarstedt), respectively. The plates were incubated at 32 °C (without shaking) for 24 h, and the rich media were replaced by MMC starvation buffer (10 mM MOPS, pH 7.6, 4 mM $MgSO_4$, 2 mM $CaCl_2$) to induce development. To enumerate developmental spores, cells were harvested from 1 well of 24-well plates in triplicate, heated to 50 °C for 60 min, sonicated (output 3, 30% duty 2× 20 pulses, Branson Sonifier 250), and then enumerated using a Helber bacterial counting chamber (Hawksley, UK).

Construction of M. xanthus Mutant Strains—In-frame deletions and site-specific point mutations were generated by homologous recombination of the relevant suicide plasmids followed by *galK*-mediated counter-selection on galactose (44), as described previously in detail (42). All strains were confirmed by sequence analyses of the relevant region (~1000 bp surrounding the desired substitution/deletion). Specific plasmids used to generate the respective strains are listed in supplemental Table S1. With the exception of pAS036 (see below), all inserts for the mutagenesis plasmids were generated accord-

TABLE 1
Strains and plasmids used in this study

Strain/plasmid	Genotype	Source
***M. xanthus* strains**		
DZ2	Wild type	67
DZ4227	DZ2 Δ*espA*	37
PH1008	DZ2 $espA_{H407A}$	36
PH1009	DZ2 $espA_{D696A}$	36
PH1029	PH1009 $espA_{H407A}$	This study
PH1044	DZ2 Δ*espC*	This study
PH1026	DZ2 $espC_{H461A}$	This study
PH1027	DZ2 $espC_{D749A}$	This study
PH1028	PH1026 $espC_{D749A}$	This study
PH1047	DZ4227 Δ*espC*	This study
PH1032	DZ2 $espC_{\Delta CA}$	This study
PH1033	PH1027 $espC_{\Delta CA}$	This study
PH1034	DZ2 $espC_{N465Y}$	This study
PH1035	PH1027 $espC_{N465Y}$	This study
PH1036	DZ2 $espC_{N465E}$	This study
PH1037	PH1027 $espC_{N465E}$	This study
PH1038	DZ2 $espC_{N465R}$	This study
PH1039	PH1027 $espC_{N465R}$	This study
PH1040	DZ2 $espC_{N465C}$	This study
PH1041	PH1027 $espC_{N465C}$	This study
PH1042	DZ2 $espC_{E462A}$	This study
PH1043	PH1027 $espC_{E462A}$	This study
PH1045	DZ2 $espA_{D411N}$	This study
***E. coli* strains**		
Top10	F$^-$ *endA1 recA1 galE15 galK16 nupG rpsL* Δ*lacX74* Φ80*lacZ*ΔM15 *araD139* Δ(ara, leu)7697 *mcrA* Δ(*mrr-hsdRMS-mcrBC*) λ$^-$	Invitrogen
BL21λDE3	F$^-$ *ompT gal dcm lon* $hsdS_B$ (r_B^- m_B^-)λ (DE3 [*lacI lacUV5*-T7 gene 1 *ind1 sam7 nin5*])	Novagen
Mutagenesis plasmids		
pBJ114	Suicide plasmid with *Km*^{R} and *galK*	68
pET24a+	T7-promotor, His_6 tag (C-terminal), *Km*^{R}	Novagen
pBS131	pBJ114 *espC* (Δcodons 44–797)	This study
pPH150	pBJ114 $espA_{H407A}$	36
pAS001	pBJ114 $espC_{H461A}$	This study
pAS004	pBJ114 $espC_{D749A}$	This study
pAS029	pBJ114 $espC_{\Delta CA}$ (Δcodons 529–674)	This study
pAS031	pBJ114 $espC_{N465Y}$	This study
pAS030	pBJ114 $espC_{N465E}$	This study
pAS032	pBJ114 $espC_{N465R}$	This study
pAS033	pBJ114 $espC_{N465C}$	This study
pAS034	pBJ114 $espC_{E462A}$	This study
pAS036	pBJ114 $espA_{D411N}$	This study
Overexpression plasmids		
pAS002	pET24a+ $espC_{\Delta MASE1}$ (aa 311–833)	This study
pBS122	pET24a+ $espC_{REC}$ (aa 690–819)	This study
pAS019	pET24a+ $espC_{REC\ D749A}$ (aa 690–819)	This study
pBS121	pET24a+ $espC_{HK}$ (aa 451–679)	This study
pAS021	pET24a+ $espC_{HK\ H461A}$ (aa 451–679)	This study
pAS022	pET24a+ $espA_{HK}$ (aa 390–646)	This study
pAS023	pET24a+ $espA_{HK\ H407A}$ (aa 390–646)	This study

ing to the detailed protocol in Ref. 42 using DZ2 genomic DNA as template and the respective primers listed in supplemental Table S2. For pBS131 (Δ*espC*), the insert was cloned into the XhoI/BamHI sites of pBJ114. For all other mutagenesis plasmids, the insert was cloned into the EcoRI/BamHI sites of pBJ114. Plasmid pAS036 ($espA_{N411D}$) was generated using a "one-step directed mutagenesis" PCR protocol (45) with outward-facing mutagenesis primers (supplemental Table S2) and pAS035 as a template. pAS035 contains codons 240–571 of *espA* cloned into pBJ114. All plasmids were sequenced to confirm the absence of PCR-generated errors.

Bioinformatic Analyses—Orthologs for EspA and EspC in the publicly available *Myxococcales* genomic sequences were identified using reciprocal BlastP analysis as described by Huntley *et al.* (18). Briefly, the protein sequence of either EspA or EspC was used as query in BlastP analysis against the protein database from the following: *Stigmatella aurantiaca* DW4/3-1 (accession number CP002271) (18); *Myxococcus fulvus* HW-1 (accession CP002830) (46); *Corallococcus coralloides* DSM2259 (accession CP003389) (19); *Anaeromyxobacter dehalogenans* 2CP-C (accession CP000251.1) (47); *Haliangium ochraceum* SMP-2 (accession CP001804.1) (48); *Sorangium cellulosum* So ce 56 (accession AM746676) (17), and *Plesiocystis pacifica* SIR-1 (accession ABCS00000000). The protein with the best hit (highest bit score) was then used as a query in a second BlastP analysis against the protein database from *M. xanthus* DK1622 (accession CP000113) (16). If the highest scoring match was identical to the protein sequence originally used for the first BlastP analysis, the two proteins were considered orthologs.

Construction of Protein Overproduction Plasmids—Protein overproduction plasmids and the primer sequences used to generate them are listed in Table 1 and supplemental Table S2, respectively. Overproduction plasmids pAS022 ($EspA_{HK}$-His_6) and pAS023 ($EspA_{HK\ H407A}$-His_6) encode the DHp and CA domains (collectively referred to as the kinase region (HK)) of *espA* with a C-terminal hexahistidine (His_6) affinity tag.

pAS022 and pAS023 were constructed by PCR amplifying the *espA* (MXAN_0931) codons 390–646 from DZ2 or PH1008 genomic DNA, respectively, and cloned into the EcoRI site of pET24a+. The resulting plasmids were restricted with SacI; overhangs were blunted with T4 DNA polymerase (Fermentas) and religated to bring the His_6 affinity tag in-frame with the $espA_{HK}$ fragment. Overproduction plasmids pBS121 ($EspC_{HK}$-His_6) and pAS021 ($EspC_{HK\ H461A}$-His_6) encode the HK of EspC and kinase-inactive point mutant with C-terminal His_6 affinity tags and were constructed by PCR-amplifying *espC* (MXAN_6855) codons 451–679 from DZ2 or PH1026 genomic DNA, respectively. The resulting fragments were cloned into the EcoRI and XhoI sites of pET24a+. Overproduction plasmids pBS122 ($EspC_{REC}$-His_6) and pAS019 ($EspC_{REC\ D749A}$-His_6) encode the REC of *espC* with a C-terminal His_6 affinity tag and were constructed by PCR-amplifying *espC* codons 690–819 from DZ2 or PH1027 genomic DNA, respectively. The resulting fragments were cloned into the EcoRI and XhoI sites of pET24a+. All constructs were sequenced to confirm absence of PCR-generated errors.

Overproduction and Purification of Recombinant Proteins—$EspA_{HK}$-His_6 or $EspC_{HK}$-His_6 (and the respective point mutants) were each produced as inclusion bodies (IBs) from 1 liter of *E. coli* BL21(λDE3) cultures by induction with 0.5 mM isopropyl 1-thio-β-D-galactopyranoside for 3 h at 37 °C. To isolate IBs, the respective cell cultures were resuspended in 25 ml of TND buffer (50 mM Tris-HCl, pH 8.0, 150 mM NaCl, 1 mM DTT) and lysed by passage through a French press (SLM-AMINCO/Spectronic) three times at ~18,000 p.s.i. IBs were collected by centrifugation at 4600 × *g* for 30 min at 4 °C, resuspended in 25 ml of TND buffer, and treated by French press as above. To remove contaminating proteins, IBs were pelleted as described above and resuspended in 20 ml of TND buffer. Guanidine HCl was added to a final concentration of 1 M, and the solution was incubated for 2 h at RT with rotation. Purified IBs were pelleted as above, washed in TND buffer, and then resuspended in 15 ml of TND buffer. Guanidine HCl was added to a final concentration of 6 M, and the IB protein was solubilized by vortexing and then clarified by centrifugation at 100,000 × *g* for 30 min at RT. The solution was diluted with TND buffer to achieve a guanidine HCl final concentration of 2 M and a protein concentration of ~0.1 mM as determined by the absorbance at 280 nm (A_{280}) (ϵ_{280}($EspA_{HK}$-His_6) = 1490; ϵ_{280}($EspC_{HK}$-His_6) = 2980). The solution was then dialyzed in TGND buffer (50 mM Tris-HCl, pH 8.0, 10% (v/v) glycerol, 150 mM NaCl, 1 mM DTT) for 2 h at 4 °C, two times, followed by dialysis in fresh buffer overnight. The resulting protein preparation was clarified by centrifugation at 17,000 × *g* for 5 min at 4 °C and concentrated using a 10 molecular weight cut-off Amicon Ultra column (Millipore). The refolded proteins were stored at −20 °C for further assays.

$EspC_{REC}$-His_6 (and its respective point mutant) were overproduced as soluble proteins in *E. coli* strain BL21(λDE3) by induction with 1 mM isopropyl 1-thio-β-D-galactopyranoside for 2 h at 37 °C. For purification of the recombinant proteins, the cell cultures were resuspended in lysis buffer (50 mM HEPES, 0.5 M NaCl, 20 mM imidazole, pH 7.4) and lysed by French press as described above. The lysate was clarified by centrifugation at 100,000 × *g* for 1 h at 4 °C, and the supernatant was subjected to purification by nickel affinity chromatography at 4 °C (ÄKTA purifier, GE Healthcare) using a 1-ml His trap FF1 nickel affinity column (Amersham Biosciences). The proteins were eluted using a 30-ml linear gradient of 20–500 mM imidazole in lysis buffer. A portion of each eluted fraction was analyzed by SDS-PAGE. Elution fractions containing the peak levels of purified protein were pooled, dialyzed, and stored as described above.

Radiolabeled in Vitro Autophosphorylation and Phosphotransfer Assays—In vitro autophosphorylation of 10 μM kinase was carried out in phosphorylation buffer (TGND buffer, 5 mM $MgCl_2$, 50 mM KCl) supplemented with 0.5 mM ATP and 1.7 μM [γ-^{32}P]ATP (222 TBq mmol^{-1}; Hartmann Analytic, Braunschweig) for intervals between 0 and 60 min. At each time point, 10 μl samples were withdrawn, quenched with 2× LSB (125 mM Tris-HCl, 20% (v/v) glycerol, 4% (w/v) SDS, 10% β-mercaptoethanol, 0.02% (w/v) bromphenol blue), and analyzed as described previously (36), except 15% polyacrylamide gels were used to resolve radiolabeled proteins. The gels were exposed to a Storage Phosphor Screen (GE Healthcare) overnight and analyzed using a Storm™ 800 imaging system (Amersham Biosciences). ^{32}P-Labeled HK signal intensities from three independent experiments were quantified by ImageQuant (GE Healthcare) with local average background correction and manual background subtraction. The average intensity and associated standard deviation were calculated using Microsoft Excel.

Phosphotransfer reactions were performed by first autophosphorylating 15 μM of either $EspA_{HK}$-His_6 or $EspC_{HK}$-His_6 (or respective point mutants) for 30 min. 6.5 μl of the HK~P were then added to 3.5 μl of either phosphorylation buffer, 28 μM $EspC_{REC}$-His_6 or $EspC_{REC\ D749A}$-His_6, leading to an equivalent 10 μM final concentration for each reaction partner. The reactions were quenched after 2 min and analyzed as above, except 20% polyacrylamide gels were used.

Immunoblot Analysis—Protein lysates for immunoblot analyses were prepared from developmental cells grown in 16 ml of submerged culture format. At the indicated time points, the MMC buffer was removed, and the cells were resuspended in 1 ml of ice-cold MMC buffer incubated with an equivalent volume of 26% ice-cold trichloroacetic acid for 15 min on ice, pelleted at 17,000 × *g* for 5 min at 4 °C, and washed twice with acetone. The pellet was resuspended in 1× clear LSB (62.5 mM Tris-HCl, 10% (v/v) glycerol, 2% (w/v) SDS) and heated for 1 min at 94 °C. The protein concentration of each sample was determined using a BCA protein assay kit (Thermo Scientific) according to manufacturer's instructions. Samples were diluted in 2× LSB to 2 μg μl^{-1} and stored at −20 °C.

For immunoblot analysis, samples containing 20 μg of protein were resolved by denaturing SDS-PAGE in 8% (anti-EspA and -EspC immunoblots) or in 12% (anti-MrpC immunoblots) polyacrylamide gels. Proteins were transferred to a PVDF membrane using a semi-dry transfer apparatus. Western blot analyses were performed using anti-EspC (supplemental Methods), anti-EspA (41), or anti-MrpC (26) primary antibodies at dilutions of 1:200, 1:1000, or 1:2000, respectively. Goat α-rabbit IgG conjugated to horseradish peroxidase (HRP) secondary anti-

body (Pierce) was used at a dilution of 1:20,000, and signals were detected with enhanced chemiluminescence substrate (Pierce) followed by exposure to autoradiography film (Thermo Scientific) or detected by LAS 4000 (Fujifilm Life Science). Representative immunoblot patterns are shown, but similar patterns were obtained from at least two biological replicates.

In Vivo MrpC Turnover Assays—Wild type (DZ2) or Δ*espA* Δ*espC* mutant (PH1047) strains were developed in 16 ml of submerged culture format for 9 h and treated with 34 μg ml^{-1} chloramphenicol to block *de novo* protein synthesis (50). At 0, 10, 20, or 30 min after addition of chloramphenicol, the cells were harvested, pelleted at 4,600 × *g* for 2 min at 4 °C, resuspended in 400 μl of hot (70 °C) LSB, heated for 5 min at 99 °C, and stored at −20 °C for further analyses. 15 μl of protein samples were analyzed by immunoblot as described above. Band intensities from triplicate experiments were quantified with ImageJ 1.43U (49). The MrpC half-life in wild type cells was calculated assuming a first order kinetic degradation reaction (51–53). Briefly, each background-subtracted band intensity value was first normalized to the intensity at $t = 0$, and the natural log of the resulting values were plotted *versus* time in Microsoft Excel. The slope (k) of a linear fit of each graph was used to calculate the $t_{1/2}$ using the equation $t_{1/2} = \ln(2)/-k$ (53).

RESULTS

EspA and EspC Function in Same Signaling Pathway—espA and *espC* each encode orphan HyHPKs and both have a similar mutant phenotype in which progression through the developmental program is accelerated relative to wild type (37, 39). To analyze whether these proteins participated in a linear signaling pathway, we took a genetic epistasis approach. We first generated isogenic Δ*espC* and Δ*espA*Δ*espC* strains and compared their developmental phenotypes to the wild type and Δ*espA* strains. The Δ*espA,* Δ*espC,* and Δ*espA*Δ*espC* strains each yielded an identical developmental phenotype; aggregation centers were visible between 12 and 24 h after induction of starvation, which was ~12 h earlier than wild type (Fig. 1*A*). Likewise, all three mutants produce heat- and sonication-resistant spores ~12 h earlier than the wild type (Fig. 1*A*). These genetic data suggest that EspA and EspC function in the same signaling pathway to regulate developmental progression.

The observation that Δ*espA*Δ*espC* double mutant phenocopied the single mutants could arise from one of two possibilities. 1) EspA regulates developmental progression, but EspC is necessary for EspA production (or vice versa). 2) EspA and EspC act together to regulate developmental progression. To distinguish between these two possibilities, we examined EspA and EspC production patterns by immunoblot analysis of cell lysates prepared from wild type, Δ*espA*, or Δ*espC* stains. The anti-EspC immunosera generated in this study could specifically detect an ~89-kDa band (similar to the predicted EspC molecular mass of ~88 kDa) in the wild type, but not Δ*espC,* lysates (Fig. 1*B*). EspC was not detected at $t = 0$, but began to accumulate at ~12 h, peaked at ~30 h, and then began to decrease, similar to the EspA accumulation pattern (Fig. 1*B*). EspC and EspA were present in the Δ*espA* and Δ*espC* strains, respectively, and accumulated earlier in the respective backgrounds than in the wild type (Fig. 1*B*). Together, these data

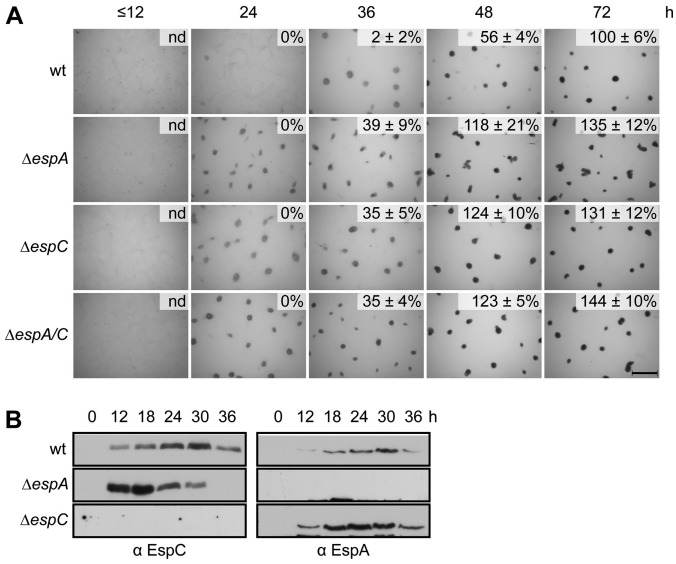

FIGURE 1. **EspA and EspC are components of a single signaling pathway.** *A*, developmental phenotypes of *esp* null mutants. Wild type (*wt*; DZ2), Δ*espA* (DZ4227), Δ*espC* (PH1044), and Δ*espA* Δ*espC* (PH1047) strains were developed under submerged culture in 24-well culture dishes, and pictures were recorded at the indicated hours of development. Heat- and sonication-resistant spores were isolated at the indicated time points and displayed as the percent of wild type spores at 72 h. Spore numbers are the average and associated standard deviation of three biological replicates. *Scale bar,* 0.5 mm; *nd,* not determined. *B*, EspA and EspC developmental protein accumulation patterns. Anti-EspC (*left*) and anti-EspA (*right*) immunoblot analysis of cell lysates prepared from the indicated strains developed for the indicated hours under 16 ml of submerged culture format.

suggest that EspA and EspC act together to regulate developmental progression. Additionally, this dual activity might, directly or indirectly, repress the accumulation of both proteins.

EspA and EspC share 48 and 40% identity in their HK and REC regions, respectively (Fig. 2). These two proteins are not paralogs, because at least three proteins (encoded by Mxan_0195, Mxan_2386, and Mxan_0095) can be identified that display a higher degree of conservation to EspA than does EspC. Orthologs to EspA and EspC can be identified in *S. aurantiaca* (STAUR_7060 and STAUR_0999, respectively), *C. coralloides* (COCOR_00882 and COCOR_07432, respectively), and *M. fulvus* (LILAB_04045 and LILAB_12195, respectively), but orthologs for neither protein could be identified in *A. dehalogenans*, *H. ochraceum*, *P. pacifica*, or *S. cellulosum*. Thus, if EspA was identified in a genome, then EspC was always additionally present, consistent with a single Esp signaling module in which both proteins act together.

espC$_{D749A}$ *but Not espC*$_{H461A}$ *Mutants Effect Developmental Progression*—We have previously demonstrated that both EspA autophosphorylation and phosphotransfer to its associated receiver domain are necessary for appropriate developmental progression; alanine substitution of the kinase autophosphorylation site (H407A) or receiver phosphoaccepting site (D696A) leads to the null mutant phenotype (36) (Fig. 3*A*). Consistently, we observed an identical phenotype if both residues in *espA* were mutated (*espA*$_{H407A,D696A}$) (Fig. 3*A*). To determine whether EspC kinase activity is similarly necessary for regulation of developmental progression, we likewise generated an alanine substitution of the predicted autophosphorylation site

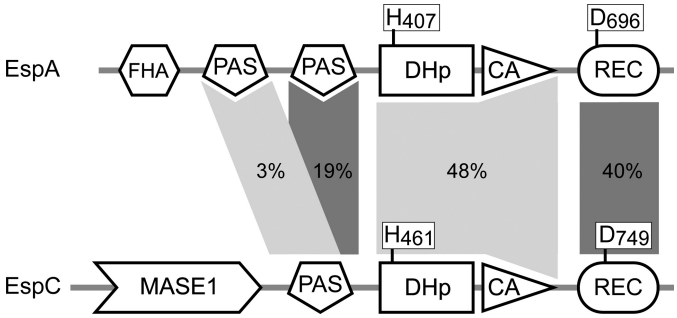

FIGURE 2. **Domain organization of the EspA and EspC hybrid histidine kinases.** Percent amino acid identity for the indicated domains is represented by *shaded areas*. The invariant histidine (*H*) residues in the dimerization and histidine phosphotransfer domains (*DHp*) and invariant aspartate (*D*) residues in the receiver (*REC*) domains are indicated. *FHA*, forkhead-associated domain; *MASE1*, predicted integral membrane sensory domain.

(His-461) in EspC ($espC_{H461A}$). Surprisingly, this mutant exhibited the wild type phenotype with respect to timing of aggregation and production of heat- and sonication-resistant spores (Fig. 3*A*). In contrast, alanine substitution of the conserved phosphoaccepting residue (Asp-749) in the receiver domain of EspC ($espC_{D749A}$) resulted in the Δ*espC* phenotype (Fig. 3*A*). An identical mutant phenotype was also observed in a strain in which both EspC His-461 and Asp-749 were substituted with alanine ($espC_{H461A,D749A}$) (Fig. 3*A*).

To determine whether the generated point mutations adversely affect the protein accumulation patterns of either EspA or EspC, we analyzed developmental cell lysates generated from the respective strains by anti-EspC and anti-EspA immunoblot analysis. Neither EspC nor EspA protein accumulation was reduced in the $espC_{H461A}$,$espC_{D749A}$ or $espC_{H461A,D749A}$ strains (Fig. 3*B*). Thus, the phenotypes observed are due to disruption of the activity of the mutated proteins rather than to reduction of protein stability for EspA or EspC. The *espC* mutants that displayed the early developmental phenotype ($espC_{D749A}$ and $espC_{H461A,D749A}$) also displayed earlier and more rapid accumulation of both EspA and EspC; peak protein levels were detected ~12 h earlier than in the wild type (Fig. 3*B*). The $espC_{H461A}$ strain, which does not display a mutant phenotype, may cause slightly earlier production of both $EspC_{H461A}$ and EspA. However, both the rate of accumulation and time point of peak production matched that of the wild type (Fig. 3*B*). Together, these results suggest that although phosphorylation of the EspC receiver is necessary for appropriate developmental regulation, the phosphoryl group is not donated from EspC kinase.

EspC Autophosphorylates on His-461 in Vitro—To ascertain whether EspC is capable of autophosphorylation *in vitro*, we next cloned, overproduced, and purified a recombinant version of the EspC-predicted histidine kinase region (aa 451–679) fused at the C terminus with a hexahistidine affinity tag ($EspC_{HK}$-His_6). We also generated a phosphorylation-deficient H461A version of this protein ($EspC_{HK\ H461A}$-His_6). As we were unable to find conditions for soluble overproduction, both proteins were refolded from inclusion bodies. To examine whether these two proteins could autophosphorylate, 10 μM of either $EspC_{HK}$-His_6 or $EspC_{HK\ H461A}$-His_6 was incubated in the presence of [γ-^{32}P]ATP for 60 min and resolved by electrophoresis,

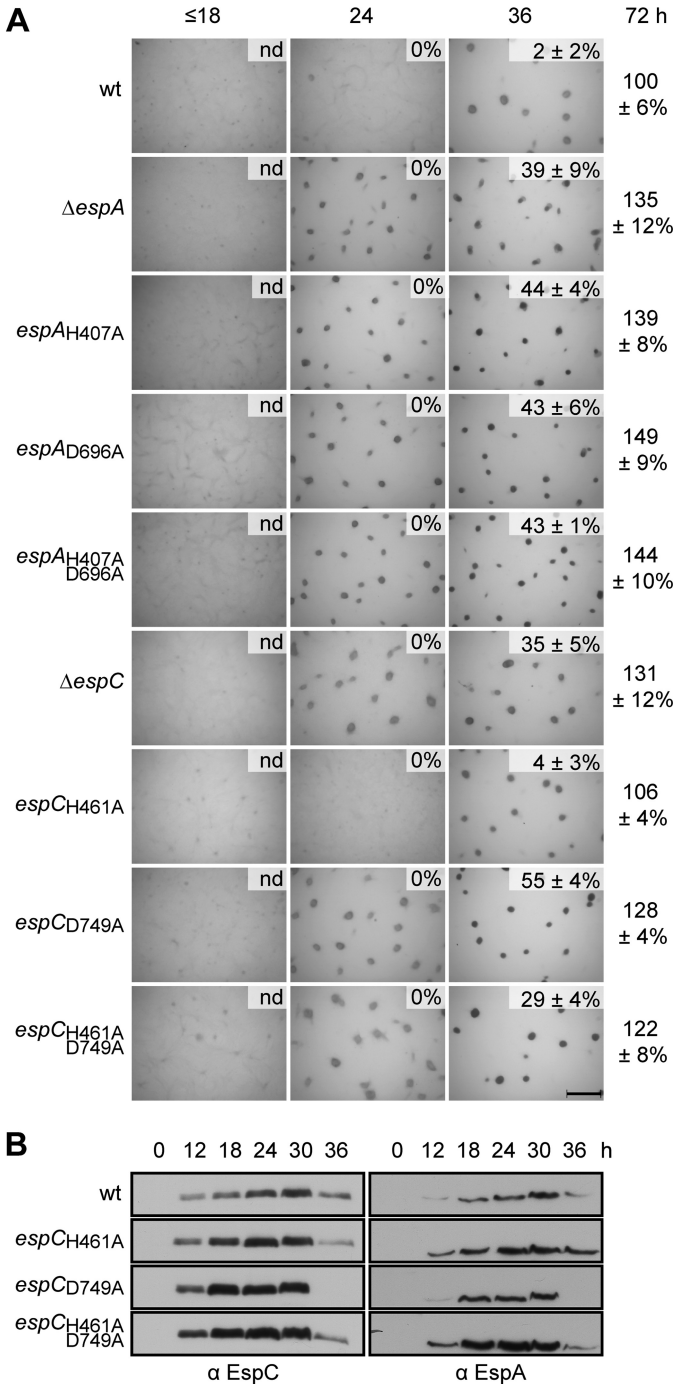

FIGURE 3. **Phosphorylation of EspC receiver domain, but not EspC autophosphorylation, is required for regulation of development.** *A*, developmental phenotypes of *espA* and *espC* signal transmission point mutants. Wild type (*wt*; DZ2), Δ*espA* (DZ4227), $espA_{H407A}$ (PH1008), $espA_{D696A}$ (PH1009), $espA_{H407A,D696A}$ (PH1029), Δ*espC* (PH1044), $espC_{H461A}$ (PH1026), $espC_{D749A}$ (PH1027),and $espC_{H461A,D749A}$ (PH1028) strains were developed under submerged culture in 24-well culture dishes, and pictures were recorded at the indicated hours of development. Heat- and sonication-resistant spores were isolated at the indicated time points and displayed as the percent of wild type spores at 72 h. Spore numbers are the average and associated standard deviation of three biological replicates. *Scale bar,* 0.5 mm; *nd,* not determined. *B*, EspC and EspA developmental protein accumulation patterns. Anti-EspC (*left panel*) and anti-EspA (*right panel*) immunoblot analyses of cell lysates were prepared from the indicated strains developed for the indicated hours under 16 ml of submerged culture format.

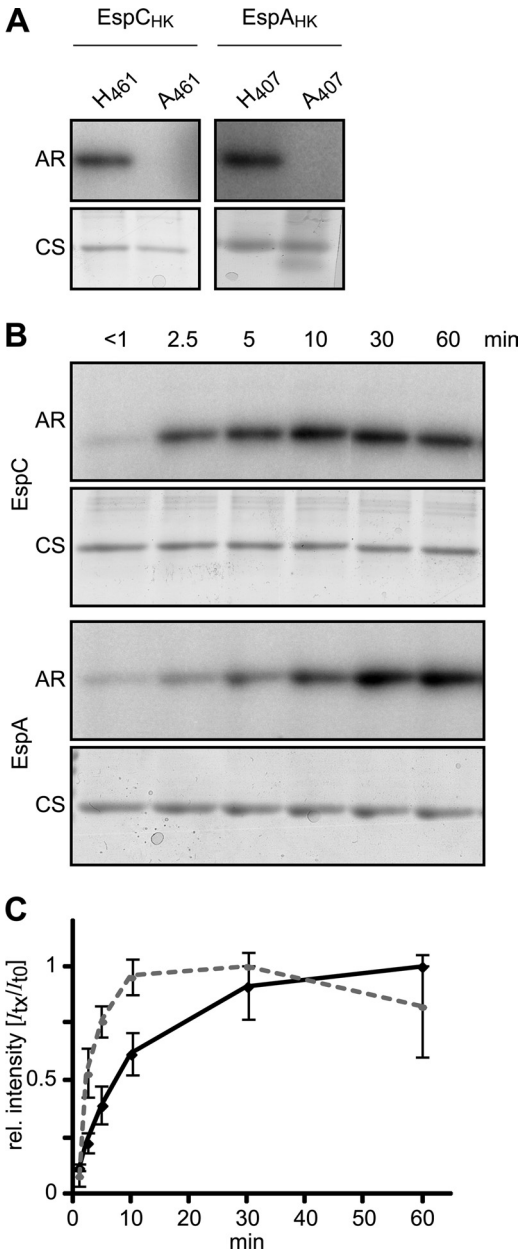

FIGURE 4. **EspC kinase region autophosphorylates *in vitro*.** *A*, *in vitro* autophosphorylation of EspA$_{HK}$-His$_6$, EspC$_{HK}$-His$_6$, EspA$_{HK\ H407A}$-His$_6$, and EspC$_{HK\ H461A}$-His$_6$. 10 μM of each recombinant protein was incubated in the presence of [γ-^{32}P]ATP for 60 min, quenched, and resolved by SDS-PAGE, and the radiolabel was detected by exposure to a Storage PhosphoScreen (*AR*). Total protein was subsequently detected by Coomassie stain (*CS*). *B*, relative *in vitro* autophosphorylation rates of EspC and EspA kinase regions. 10 μM EspA$_{HK}$-His$_6$ or EspC$_{HK}$-His$_6$ was incubated in the presence of [γ-^{32}P]ATP; aliquots were removed at the indicated time points and analyzed as above. *C*, quantification of EspC (*dashed line*) and EspA (*solid line*) HK autophosphorylation rates in *B*. Relative (*rel.*) signal intensities of the bands from three independent time courses were quantified and normalized to the maximal signal intensity of each protein. The average relative signal intensity and associated standard deviation from each time point was plotted.

and radioactive incorporation onto either protein was analyzed by exposure to a phosphor-imager screen. A radiolabeled band corresponding to EspC$_{HK}$-His$_6$, but not EspC$_{HK\ H461A}$-His$_6$, could be detected (Fig. 4*A*), suggesting that the EspC kinase region is capable of *in vitro* autophosphorylation on His-461.

To compare the relative activities of the EspC and EspA kinase domains, we generated comparable constructs to produce EspA$_{HK}$-His$_6$ (aa 390–646) or the kinase-deficient EspA$_{HK\ H407A}$-His$_6$. Although these two recombinant proteins could be overproduced as soluble proteins, they were denatured and refolded as for the EspC kinase constructs. As observed previously for a GST-EspA$_{HK}$ construct (36), EspA$_{HK}$-His$_6$, but not EspA$_{HK\ H407A}$-His$_6$, could be labeled by ^{32}P (Fig. 4*A*). To compare EspA$_{HK}$-His$_6$ and EspC$_{HK}$-His$_6$ activity *in vitro*, 10 μM of the respective proteins was incubated in the presence of [γ-^{32}P]ATP for intervals between ~0 and 60 min (Fig. 4, *B* and *C*). In the case of EspC$_{HK}$-His$_6$, ^{32}P incorporation could be detected after less than 1 min, and the signal continued to accumulate for 30 min, after which it began to decrease. EspA$_{HK}$-His$_6$ exhibited slower accumulation of the ^{32}P label that began to saturate between 30 and 60 min of incubation (Fig. 4, *B* and *C*). Together, these results indicate that the EspC kinase region is capable of efficient autophosphorylation *in vitro* with greater activity than that of EspA, despite the observation that the kinase activity is apparently not required during development *in vivo*.

EspA$_{HK}$ but Not EspC$_{HK}$ Can Transfer a Phosphoryl Group to EspC$_{REC}$ in Vitro—To test our hypothesis that EspA, and not EspC, acts as the phosphodonor to EspC$_{REC}$, we examined phosphotransfer between EspA$_{HK}$ or EspC$_{HK}$ to the EspC receiver domain *in vitro*. For this purpose, the EspC receiver domain (aa 690–819), or the putative phosphoaccepting deficient version was each overproduced with C-terminal hexahistidine affinity tags (EspC$_{REC}$-His$_6$ or EspC$_{REC\ D749A}$-His$_6$, respectively). To first examine whether EspC$_{HK}$ could phosphorylate its own receiver *in vitro*, we allowed for kinase autophosphorylation by incubating EspC$_{HK}$-His$_6$ (or the EspC$_{HK\ H461A}$-His$_6$ control) with [γ-^{32}P]ATP for 30 min. We next added the kinase to either buffer alone or to an equimolar (10 μM) concentration of either EspC$_{REC}$-His$_6$ or EspC$_{REC\ D749A}$-His$_6$ and allowed phosphotransfer reactions to proceed for 2 min. As expected, if either EspC$_{HK}$-His$_6$ or EspC$_{HK\ H461A}$-His$_6$ was first autophosphorylated and subsequently incubated only with buffer, the ^{32}P signal was readily detected on the wild type, but not on the mutated, kinase (Fig. 5, *A* and *B, lanes 1* and *2*). If the kinase was instead added to either EspC$_{REC}$-His$_6$ or EspC$_{REC\ D749A}$-His$_6$, no significant change in signal incorporation on EspC$_{HK}$-His$_6$ could be observed, and no significant ^{32}P label could be detected on either receiver construct (Fig. 5, *A* and *B, lanes 3–5*). These results suggest EspC$_{HK}$-His$_6$ does not act as an efficient phosphodonor for its own receiver *in vitro*.

We next performed this experiment substituting EspA$_{HK}$ for that of EspC$_{HK}$. As expected, if either EspA$_{HK}$-His$_6$ or EspA$_{HK\ H407A}$-His$_6$ was first autophosphorylated and subsequently incubated only with buffer, the ^{32}P signal was readily detected on the wild type but not on the mutated kinase (Fig. 5, *A* and *B, lanes 6* and *7*). In contrast, if EspC$_{REC}$-His$_6$ was substituted for the buffer, the signal intensity on EspA$_{HK}$-His$_6$ was reduced to 16 ± 5, and 8 ± 1% of the original kinase signal could be clearly detected on EspC$_{REC}$-His$_6$ (Fig. 5, *A* and *B, lane 8*). These effects were not observed if the kinase was instead added to EspC$_{REC\ D749A}$-His$_6$ (Fig. 5, *A* and *B, lane 10*) or if EspA$_{HK\ H407A}$-His$_6$ was added instead of the functional HK (Fig. 5, *A* and *B, lane 9*). These results indicate that the EspA kinase region can efficiently phosphorylate the receiver of EspC

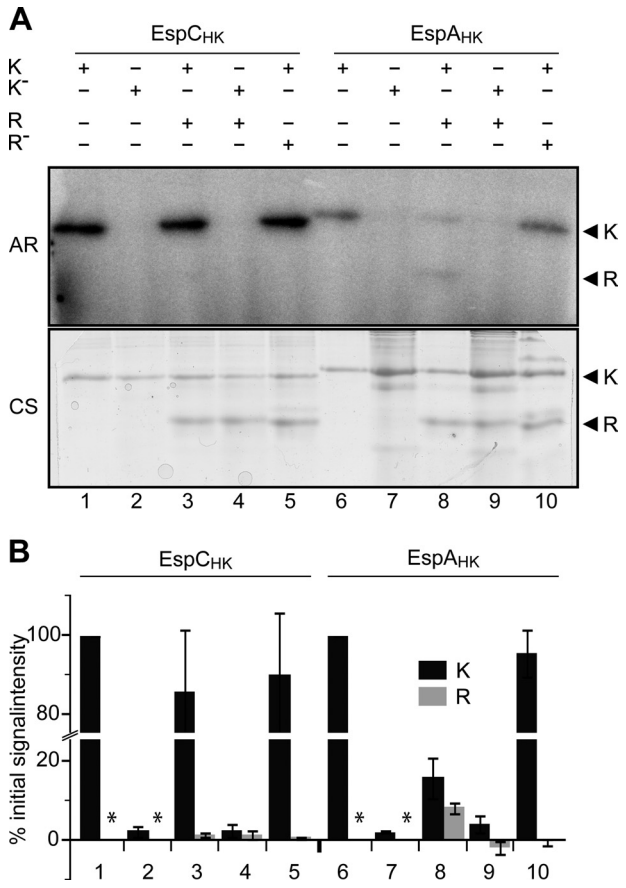

FIGURE 5. **EspA$_{HK}$, but not EspC$_{HK}$, efficiently phosphorylates EspC$_{REC}$.** *A, in vitro* phosphotransfer from autophosphorylated EspC or EspA kinase regions to EspC receiver domain (*EspC$_{REC}$*). *Lanes 1–5,* EspC$_{HK}$-His$_6$ (*K*) or EspC$_{HK\ H461A}$-His$_6$ (*K*$^-$) was first incubated in the presence of [γ-^{32}P]ATP for 30 min and then incubated with either buffer or equimolar (10 μM) EspC$_{REC}$-His$_6$ (*R*) or EspC$_{REC\ D749A}$-His$_6$ (*R*$^-$) for 2 min as indicated. +, indicated component present; −, indicated component absent. *Lanes 6–10,* EspA$_{HK}$-His$_6$ (*K*) or EspA$_{HK\ H407A}$-His$_6$ (*K*$^-$) analyzed as per *lanes 1–5*. All samples were quenched and resolved by SDS-PAGE, and radiolabel was detected by exposure to a Storage PhosphoScreen (*AR*). Total protein was subsequently detected by Coomassie stain (*CS*). *B,* quantification of the relative signal intensities of radiolabeled EspC or EspA HK (*K, black bars*), and EspC$_{REC}$ (*R, gray bars*). Signal intensities are the average and associated standard deviation of three biological replicates of the reactions represented in *A*. HK and REC intensity values are reported as a percent of the respective Esp HK autophosphorylation controls (represented by *lanes 1* and *6*, respectively). *, not determined.

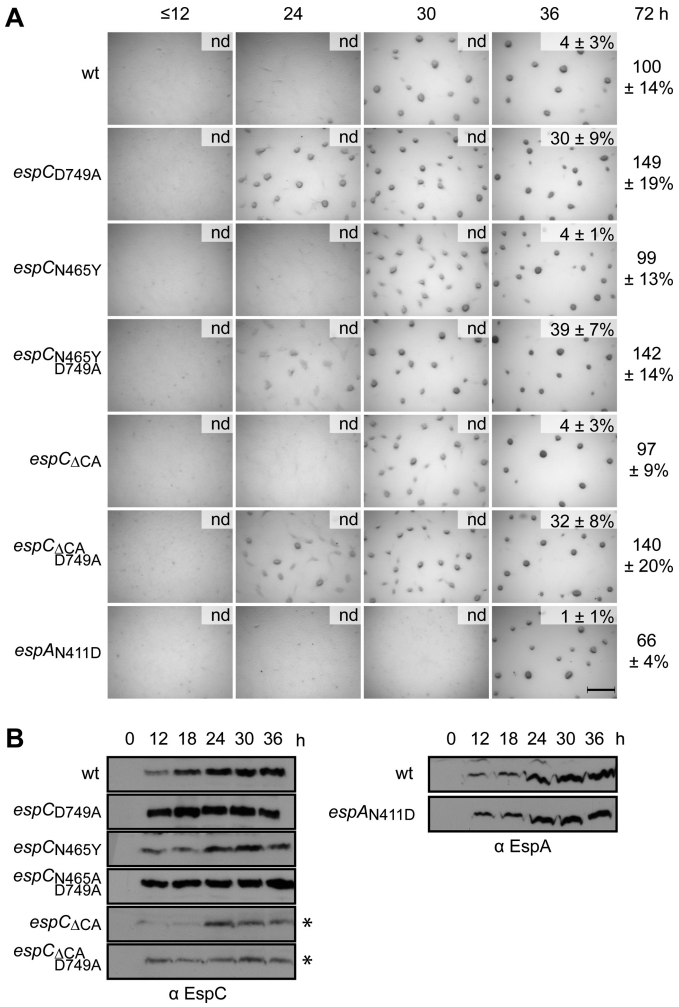

FIGURE 6. **Disruption of a phosphatase motif in EspA but not EspC effects developmental progression.** *A*, developmental phenotypes of *espC* and *espA* phosphatase motif mutants. Wild type (*wt*; DZ2), *espC*$_{D749A}$ (PH1027), *espC*$_{N465Y}$ (PH1034), *espC*$_{N465Y,D749A}$ (PH1035), *espC*$_{\Delta CA}$ (PH1032), espC$_{\Delta CA,D749A}$ (PH1033), and *espA*$_{N411D}$ (PH1045) strains were developed under submerged culture in 24-well culture dishes, and pictures were recorded at the indicated hours of development. Heat- and sonication-resistant spores were isolated at the indicated time points and displayed as the percent of wild type spores at 72 h. Spore numbers are the average and associated standard deviation of three biological replicates. *Scale bar,* 0.5 mm; *nd*, not determined. *B*, EspC and EspA developmental protein accumulation patterns. Anti-EspC (*left panel*) and anti-EspA (*right panel*) immunoblot analyses of cell lysates were prepared from the indicated strains developed for the indicated hours under 16 ml of submerged culture format. *, 5 times longer exposure is required.

on its predicted phosphoaccepting residue, Asp-749, although under equivalent conditions EspC$_{HK}$ cannot.

Disruption of a Phosphatase Motif in EspA but Not EspC Delays Development—Our results so far suggested that EspC kinase activity is not necessary for regulation of developmental progression. However, many kinases also display phosphatase activity that is not necessarily disrupted by substitution of the phosphoaccepting histidine residue (9, 54, 55). We next set out to investigate whether EspC may function exclusively as a phosphatase in this system, by generating phosphatase motif (^{462}E*XX*N^{465}) substitutions that correspond to those producing reduced phosphatase activity in other bifunctional kinases (7, 56). Strains producing EspC$_{N465Y}$ displayed a phenotype indistinguishable from wild type with respect to fruiting body formation and sporulation (Fig. 6*A*), although the levels of EspC$_{N465Y}$ were slightly reduced relative to that of EspC (Fig. 6*B*). As expected, if the D749A mutation was combined with the N465Y mutation in EspC (*espC*$_{N465Y,D749A}$), the early developmental phenotype was observed, and the double mutant protein levels increased to a similar intensity of EspC$_{D749A}$ (Fig. 6*B*). Several additional substitutions in the putative phosphatase motif corresponding to substitutions producing reduced phosphatase activity in other bifunctional kinases (*espC*$_{E462A}$, *espC*$_{N465E}$, *espC*$_{N465R}$, or *espC*$_{N456C}$) displayed a developmental phenotype indistinguishable from wild type (supplemental Fig. S1*A*). If these mutations were combined with D749A, all double mutants displayed a phenotype indistinguishable from the *espC*$_{D749A}$ early developmental phenotype (supplemental Fig. S1*A*). The single mutants exhibited reduced protein levels relative to the wild type, which were increased in the double mutants (supplemental Fig. S1*B*).

Residues necessary for phosphatase activity have also previously been identified in the CA domain of some kinases, and CA activity has been shown to stimulate phosphatase activity (8, 9, 57). Therefore, we additionally deleted the entire EspC CA domain (aa 529–674) alone or in combination with the D749A mutation. The *espC*$_{\Delta CA}$ mutant displayed a phenotype indistinguishable from wild type with respect to fruiting body formation and sporulation, although the *espC*$_{\Delta CA,D749A}$ displayed the early developmental phenotype (Fig. 6*A*). EspC$_{\Delta CA}$ and EspC$_{\Delta CA,D749A}$ could be detected by anti-EspC immunoblot at a molecular mass of ~65 kDa (predicted molecular mass, 73 kDa) (Fig. 6*B*) and at reduced levels relative to wild type. The reduced intensity of these two mutants relative to EspC in the respective background strains is likely due to loss of some of the antibody epitopes in this protein; anti-EspC antisera were generated against EspC aa 311–833 such that the EspC$_{\Delta CA}$ mutants lack 28% of the antigen.

To determine whether disruption of the putative phosphatase motif in EspA (^{408}E*XX*N^{411}) would produce the delayed developmental phenotype consistent with hyper-phosphorylation of EspA and/or EspC receivers preventing developmental progression, we next analyzed the phenotype of an *espA*$_{N411D}$ mutant. This mutant began to aggregate between 30 and 36 h of development (~6 h later than the wild type) and produced 66% of wild type spores at 72 h of development.

Together, these results suggest that the putative phosphatase motif in EspA, but not EspC, is important for appropriate regulation of developmental progression. Finally, the observation that the EspC$_{\Delta CA}$ mutants display a wild type phenotype further confirms that EspC kinase activity is not necessary for *in vivo* control of the developmental progression.

EspA/C System Regulates the Protein Stability of Transcription Factor MrpC—We have previously demonstrated that EspA regulates the accumulation of the key developmental regulator MrpC, because in a Δ*espA* mutant MrpC protein, but not *mrpC* transcript, is produced earlier than in the wild type (36). Because our results suggested that EspA and EspC function together, we next examined whether EspC is also involved in regulating MrpC accumulation during development. We used anti-MrpC immunoblot analysis to compare the production of MrpC in the various *espC* mutants to the wild type. In wild type cells, MrpC could be detected immediately after induction of development ($t = 0$), decreased between 0 and 12 h, and thereafter gradually increased over at least 36 h of development (Fig. 7*A*). Consistent with what was observed previously in the Δ*espA* mutant (36), all early developing EspC mutants (Δ*espC*, *espC*$_{D749A}$, and *espC*$_{H461A,D749A}$) produced MrpC more rapidly than the wild type, with MrpC levels at 18 and 24 h higher than the wild type levels (Fig. 7*A*). In contrast, the *espC*$_{H461A}$ mutant displayed an accumulation pattern more similar to wild type, although the MrpC level is further reduced at 36 h (Fig. 7*A*). Taken together, these results suggest that phosphorylation of both EspA and EspC is necessary for appropriate MrpC accumulation during development.

Given that the *mrpC* transcriptional pattern in *espA* mutants matched that of wild type (36), we postulated that the Esp system either effected translation or proteolytic turnover of MrpC. If MrpC is subject to proteolytic turnover, we would predict

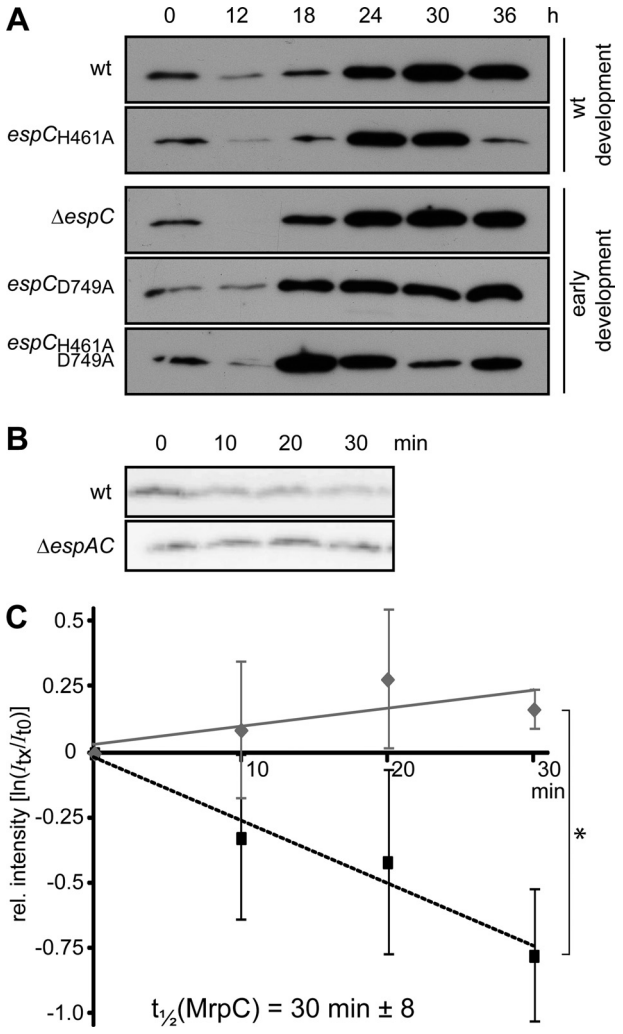

FIGURE 7. **Esp system negatively regulates MrpC protein stability.** *A,* MrpC developmental protein accumulation patterns in the wild type (DZ2, *wt*), Δ*espC* (PH1044), Δ*espA* Δ*espC* (PH1047), *espC*$_{H461A}$ (PH1026), *espC*$_{D749A}$ (PH1027), and *espC*$_{H461A,D749A}$ (PH1028) strains. 10 μg of total protein lysates developed for the indicated hours in the 16-ml submerged culture format were subject to anti-MrpC immunoblot. *B,* chloramphenicol chase of MrpC. Wild type (*wt*) or Δ*espA* Δ*espC* cells were developed for 9 h as above and treated with 34 μg ml^{-1} chloramphenicol for the indicated minutes. Equal proportions of the samples were subject to anti-MrpC immunoblot. *C,* calculation of the half-life ($t_{1/2}$) of MrpC. Triplicate biological replicates of the wild type (*black line*) and Δ*espA* Δ*espC* (*gray line*) chloramphenicol chase experiments represented in *B* were performed, and the MrpC band intensity for each time point was normalized to $t = 0$ of the respective strain and averaged. The natural log of the average intensities was plotted *versus* min of chloramphenicol treatment and the slope a linear fit of the data were used to calculate the MrpC $t_{1/2}$ in wild type cells as described under "Experimental Procedures." No significant decrease in MrpC signal intensity could be detected in the Δ*espA* Δ*espC* strain. *Vertical bars*, standard deviation of the average from triplicate biological replicates; *, average intensity values are significantly different ($p = 0.003$).

that MrpC levels would decrease in cells in which *de novo* protein synthesis is blocked. To examine whether this is the case, we developed wild type cells for 9 h in submerged culture, treated the cells with 34 μg ml^{-1} chloramphenicol, harvested cells after 0, 10, 20, or 30 min, and examined the MrpC levels by immunoblot (Fig. 7*B*). In the wild type strain, MrpC levels decreased steadily during the 30 min of treatment with a calculated half-life of 30 ± 8 min (Fig. 7*C*). To determine whether MrpC turnover was altered in the absence of EspA and EspC,

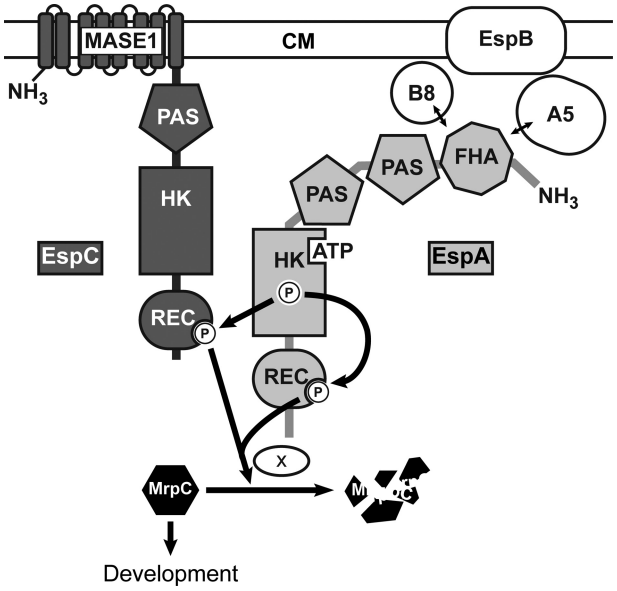

FIGURE 8. **Model of the Esp signaling system.** Two-hybrid histidine kinases EspC (*dark gray*) and EspA (*light gray*) regulate the accumulation rate of an important developmental regulator, MrpC, to ensure appropriate and coordinated progression through the *M. xanthus* developmental program. The combined phosphorylation of EspA and EspC receiver domains (*REC*) activates an unknown protease or protease targeting factor (×) to stimulate MrpC turnover. EspA histidine kinase region (*HK*) autophosphorylates and donates a phosphoryl group to both its own and EspC receiver domains. EspA may also act as a phosphatase on EspA and or EspC REC. Autophosphorylation of EspC histidine kinase domain is not required for stimulating MrpC turnover under laboratory developmental conditions. EspA activity is controlled by a signaling module consisting of two serine/threonine kinases, PktA5 (*A5*) and PktB8 (*B8*), and a putative transport protein (EspB) predicted to reside in the cytoplasmic membrane (*CM*) (37, 41). PktA5 and PktB8 are thought to interact with the Forkhead associated (*FHA*) domain in EspA (41). Two PAS domains in EspA and one in EspC may be involved in sensing internal or membrane-associated redox stimuli (65). EspC is predicted to be anchored in the CM by putative MASE1 sensing domain of unknown function (64). The array of signaling domains may allow cell fate-specific accumulation of MrpC within the developmental program.

we performed the same experiment with the Δ*espA* Δ*espC* strain. Interestingly, in this mutant, MrpC levels did not appreciably decrease (Fig. 7*B*), and quantification of the immunoblot revealed that no loss in MrpC signal was detected over 30 min of chloramphenicol treatment. Together, these results demonstrate that the MrpC protein is subject to proteolytic turnover, which is not observed in the absence of the Esp system.

DISCUSSION

EspA, EspB, PktA5, and PktB8 form an unusually complex bacterial signaling system that negatively regulates progression through the elaborate *M. xanthus* developmental program (Fig. 8) (36, 37, 41). In this study, we reveal an additional level of complexity in this system by demonstrating that a second HyHPK, EspC, is an obligate component of this system. Together, our data suggest a model in which EspA and EspC function together via an intimate hybrid histidine kinase signaling mechanism involving both an inter-HyHPK phosphorylation (from EspA kinase region to EspC receiver domain) and intra-HyHPK phosphorylation (from EspA kinase to its own receiver) (Fig. 8). The combined phosphorylation of EspA and EspC receiver domains (EspA∼P/EspC∼P) is necessary to stimulate turnover of an important developmental regulator, MrpC.

The obligatory role of EspC in this signaling system is strongly supported by the observation that the Δ*espA*, Δ*espC*, and Δ*espA* Δ*espC* mutants display identical developmental phenotypes (Fig. 1). Consistently, we observed that if an *espA* ortholog could be identified in a sequenced myxobacterial genome, we could also identify an *espC* ortholog in the same genome. Our data indicate that EspA and EspC function together via an intimate hybrid histidine kinase signaling mechanism involving both an inter- and intra-HyHPK phosphorylation. First, we determined that the EspC receiver must be phosphorylated to negatively regulate development, but that EspC kinase is not the phosphoryl donor, because inactivation of kinase autophosphorylation either by substitution of the phosphoaccepting histidine residues or deletion of the entire CA domain yields the wild type phenotype (Figs. 3 and 6). The $EspC_{HK}$ is functional because it efficiently autophosphorylates *in vitro* (Fig. 4). $EspC_{HK}$ does not, however, efficiently donate a phosphoryl group to the EspC receiver (Fig. 5). Therefore, the phosphoryl donor must either be a small molecule donor (*e.g.* the intracellular acetyl-phosphate pools (5, 58) or an alternate kinase. The former is unlikely because the EspC receiver domain does not autophosphorylate in the presence of acetyl-[^{32}P]phosphate *in vitro* (data not shown). Instead, our data suggest the phosphoryl donor is EspA kinase because of the following: 1) inactivation ($EspA_{H407A}$) produces a phenotype identical to the $EspC_{D749A}$ mutant (Fig. 3); 2) our deletion mutant analysis indicated EspA and EspC must function together (Fig. 1); and 3) $EspA_{HK\sim P}$ efficiently donates a phosphoryl group to the EspC REC *in vitro* (Fig. 5).

We suggest that the simplest interpretation of our observation of identical mutant phenotypes of the Δ*espA*, Δ*espC*, Δ*espA* Δ*espC*, $espA_{D696A}$, and $espC_{D749A}$ strains is that the output from this system is the combined phosphorylation of both EspA and EspC receiver domains (Fig. 8). Given that it has been previously observed that receiver domains can both inhibit (13) or stimulate (59) cognate kinase activities, we also considered alternate scenarios in which one of the receivers plays a phosphorylation-dependent regulatory role to modulate the kinase activity of the other. We immediately discarded scenarios in which either of the receivers inhibit EspA kinase activity, because these models predict a delayed developmental phenotype in the Δ*espC* mutant or in a mutant where the EspA receiver domain was deleted ($espA_{\Delta REC}$), and both of these mutants exhibit early development (this study and Ref. 36). We also discarded a model in which an EspA-phosphorylated receiver is the sole output, but EspA kinase-dependent phosphorylation of the EspC receiver stimulates the EspA kinase because EspA efficiently phosphorylates its own receiver *in vitro* (36). Finally, we disfavor a model in which the EspC receiver is the sole output, and phosphorylation of the EspA receiver is necessary to stimulate phosphorylation of the EspC receiver. In this last scenario, we would predict that in $espA_{D696A}$ and $espA_{\Delta REC}$ strains a low level of EspA-kinase phosphotransfer to EspC receiver would produce an intermediate phenotype rather than the null phenotypes observed in the respective mutants (Figs. 1 and 3) (36). It has also been previously proposed that kinases can form heterodimers (60). However, we do not favor a model in which EspA and EspC

form obligate heterodimers, because both EspA and EspC kinase domains are functional as individually purified proteins (Fig. 4), and we could detect $EspA_{HK}$-$EspA_{HK}$ and $EspC_{HK}$-$EspC_{HK}$, but not $EspA_{HK}$-$EspC_{HK}$, interactions by yeast two-hybrid analysis.[5] Thus, we favor the model in which EspA dimers interact with EspC dimers at minimum through the $EspA_{HK}$ and $EspC_{REC}$ domains.

Our data suggest no significant role for the $EspC_{HK}$ domain in control of developmental progression because neither substitution of the phosphoaccepting residue, deletion of the CA domain, nor mutation of several residues predicted to disrupt putative phosphatase activity produce an obvious mutant phenotype. Because we were unable to develop a system to test *in vitro* phosphatase activity of $EspC_{HK}$, we cannot test whether $EspC_{HK}$ displays phosphatase activity and whether these mutants indeed disrupt phosphatase activity. However, a disruption of this motive in *espA* ($espA_{N411D}$) produced a delayed developmental phenotype (Fig. 6) that is consistent with hyperphosphorylation of EspA and/or EspC receivers. Because the $EspC_{HK}$ module is capable of efficient autophosphorylation *in vitro*, we hypothesize that EspC kinase activity is retained because it is necessary for modulating the Esp system under conditions not triggered in the laboratory setting.

Our data suggest that the target of the Esp signaling system is the proteolytic turnover of MrpC, a key developmental transcriptional regulator that is necessary to promote aggregation of cells into fruiting bodies (31, 61), and it may play a role in programmed cell death (26, 28). MrpC transcriptional activity is thought to be negatively regulated by a serine/threonine kinase cascade and stimulated in an MrpC isoform thought to lack the 25 N-terminal amino acids (33). We and others have previously demonstrated that premature activation (34) or accumulation (36) of MrpC leads to early accumulation of the MrpC targets and produces an early developmental phenotype. The observation that MrpC accumulates inappropriately rapidly in the Δ*espA* (36) and Δ*espC* mutants (Fig. 7) is explained by the demonstration that during early development MrpC is rapidly turned over in wild type ($t_{½}$ ~30 min) but not in Δ*espA* Δ*espC* mutant cells. Given that the $espA_{D696A}$ and $espC_{D749A}$ point mutants exhibit the same phenotype as the deletion mutants, we propose that the EspA~P/EspC~P signaling state stimulates proteolytic turnover of MrpC.

We do not yet understand how EspA~P/EspC~P stimulates proteolytic turnover of MrpC, but there are several examples of regulated proteolysis controlled by RRs. For example, *E. coli* RpoS, the master regulator of the general stress response, is targeted to the ClpXP proteosome by interaction with the phosphorylated RR, RssB (62), and the *C. crescentus* single domain RR, CpdR, promotes degradation of the master regulator, CtrA, by interacting with ClpXP and promoting its localization to its target (63). We favor the hypothesis that EspA/EspC receiver domains regulate MrpC proteolysis by directly binding target proteins (*e.g.* sequestering a targeting protein in the unphosphorylated state or by recruiting MrpC together with a protease/protease targeting factor in the phosphorylated state). Alternatively, it may be that the Esp system feeds into a multistep phosphorelay involving an unidentified histidine phosphotransferase protein and soluble RR output protein.

One additional output of EspA~P/EspC~P is the repression of EspA and EspC protein accumulation, because early developing *espA* or *espC* point mutant strains also accumulate both EspA and EspC earlier than in the wild type (Figs. 1*B* and 3*B*) (36). At least in the case of the $espA_{H407A}$ mutant, early $EspA_{H407A}$ production correlates with increased *espA* transcription (36), suggesting that the system somehow additionally modulates a transcriptional regulator of *espAB* and likely *espC*. An intriguing possibility is that this transcriptional regulator is MrpC itself, leading to a negative feedback such that as long as EspA/EspC are phosphorylated their levels and MrpC levels remain low.

What is the advantage of this intricate signaling system? An obvious answer is that regulation of MrpC accumulation can be coupled to stimuli sensing domains of both EspA and EspC. This complex signal sensing capacity may be justified because different patterns of MrpC accumulation may mediate different developmental cell fate decisions in *M. xanthus* (31, 32). Perhaps different combinations of extra-cytoplasmic and cytoplasmic signals could lead the Esp system to regulate MrpC accumulation differently in cells destined for different developmental cell fates. Both Esp proteins contain multiple sensing domains; EspC contains an integral membrane MAES1 domain of unknown function (64) and a PAS domain; EspA contains a fork-head associated (FHA) domain and two PAS domains (Fig. 2). PAS domains have been implicated in binding of various diverse ligands, mediating protein interactions, protein localization, and signal transmission (65). FHA domains are protein interaction modules that recognize phosphothreonine-containing proteins (66), and the EspA FHA domain is very likely involved in binding to the kinases PktA5 and PktB8 that modulate EspA activity (41). We propose that each of these sensing domains could contribute to modulation of the level of EspA~P/EspC~P-generating cell-specific regulation of MrpC accumulation in response to temporal, spatial, and condition-specific signals. In the case of EspC, the sensing domains may regulate EspC kinase activity in response to signals not present under laboratory conditions and/or by simply regulating accessibility of EspC receiver to EspA kinase.

In summary, this study reveals a novel signaling mechanism involving two orphan HyHPKs that participate in an obligate inter- and intraphosphotransfer such that the signaling output is a combined phosphorylation of the two receiver domains. This system represents an excellent example of the inherent plasticity of the His-Asp signaling family, and in particular, it highlights HyHPKs as important players in signal integration.

Acknowledgments—We gratefully acknowledge past and present members of the Higgs group for helpful discussions. We also gratefully acknowledge Stuart Huntley and Katharina Schlereth for critical reading of the manuscript.

[5] T. Jeganathan, A. Schramm, and P. Higgs, unpublished data.

REFERENCES

1. Stock, A. M., Robinson, V. L., and Goudreau, P. N. (2000) Two-component signal transduction. *Annu. Rev. Biochem.* **69,** 183–215

2. Wuichet, K., Cantwell, B. J., and Zhulin, I. B. (2010) Evolution and phyletic distribution of two-component signal transduction systems. *Curr. Opin. Microbiol.* **13,** 219–225
3. Dutta, R., Qin, L., and Inouye, M. (1999) Histidine kinases. Diversity of domain organization. *Mol. Microbiol.* **34,** 633–640
4. Casino, P., Rubio, V., and Marina, A. (2009) Structural insight into partner specificity and phosphoryl transfer in two-component signal transduction. *Cell* **139,** 325–336
5. Lukat, G. S., McCleary, W. R., Stock, A. M., and Stock, J. B. (1992) Phosphorylation of bacterial response regulator proteins by low molecular weight phosphodonors. *Proc. Natl. Acad. Sci. U.S.A.* **89,** 718–722
6. Bourret, R. B. (2010) Receiver domain structure and function in response regulator proteins. *Curr. Opin. Microbiol.* **13,** 142–149
7. Huynh, T. N., Noriega, C. E., and Stewart, V. (2010) Conserved mechanism for sensor phosphatase control of two-component signaling revealed in the nitrate sensor NarX. *Proc. Natl. Acad. Sci. U.S.A.* **107,** 21140–21145
8. Zhu, Y., Qin, L., Yoshida, T., and Inouye, M. (2000) Phosphatase activity of histidine kinase EnvZ without kinase catalytic domain. *Proc. Natl. Acad. Sci. U.S.A.* **97,** 7808–7813
9. Jagadeesan, S., Mann, P., Schink, C. W., and Higgs, P. I. (2009) A novel "four-component" two-component signal transduction mechanism regulates developmental progression in *Myxococcus xanthus*. *J. Biol. Chem.* **284,** 21435–21445
10. Mascher, T., Helmann, J. D., and Unden, G. (2006) Stimulus perception in bacterial signal-transducing histidine kinases. *Microbiol. Mol. Biol. Rev.* **70,** 910–938
11. Galperin, M. Y. (2006) Structural classification of bacterial response regulators. Diversity of output domains and domain combinations. *J. Bacteriol.* **188,** 4169–4182
12. Posas, F., Wurgler-Murphy, S. M., Maeda, T., Witten, E. A., Thai, T. C., and Saito, H. (1996) Yeast HOG1 MAP kinase cascade is regulated by a multistep phosphorelay mechanism in the SLN1-YPD1-SSK1 "two-component" osmosensor. *Cell* **86,** 865–875
13. Inclán, Y. F., Laurent, S., and Zusman, D. R. (2008) The receiver domain of FrzE, a CheA-CheY fusion protein, regulates the CheA histidine kinase activity and downstream signalling to the A- and S-motility systems of *Myxococcus xanthus*. *Mol. Microbiol.* **68,** 1328–1339
14. Wegener-Feldbrügge, S., and Søgaard-Andersen, L. (2009) The atypical hybrid histidine protein kinase RodK in *Myxococcus xanthus*. Spatial proximity supersedes kinetic preference in phosphotransfer reactions. *J. Bacteriol.* **191,** 1765–1776
15. Wuichet, K., and Zhulin, I. B. (2010) Origins and diversification of a complex signal transduction system in prokaryotes. *Sci. Signal.* **3,** ra50
16. Goldman, B. S., Nierman, W. C., Kaiser, D., Slater, S. C., Durkin, A. S., Eisen, J. A., Eisen, J., Ronning, C. M., Barbazuk, W. B., Blanchard, M., Field, C., Halling, C., Hinkle, G., Iartchuk, O., Kim, H. S., Mackenzie, C., Madupu, R., Miller, N., Shvartsbeyn, A., Sullivan, S. A., Vaudin, M., Wiegand, R., and Kaplan, H. B. (2006) Evolution of sensory complexity recorded in a myxobacterial genome. *Proc. Natl. Acad. Sci. U.S.A.* **103,** 15200–15205
17. Schneiker, S., Perlova, O., Kaiser, O., Gerth, K., Alici, A., Altmeyer, M. O., Bartels, D., Bekel, T., Beyer, S., Bode, E., Bode, H. B., Bolten, C. J., Choudhuri, J. V., Doss, S., Elnakady, Y. A., Frank, B., Gaigalat, L., Goesmann, A., Groeger, C., Gross, F., Jelsbak, L., Kalinowski, J., Kegler, C., Knauber, T., Konietzny, S., Kopp, M., Krause, L., Krug, D., Linke, B., Mahmud, T., Martinez-Arias, R., McHardy, A. C., Merai, M., Meyer, F., Mormann, S., Muñoz-Dorado, J., Perez, J., Pradella, S., Rachid, S., Raddatz, G., Rosenau, F., Rückert, C., Sasse, F., Scharfe, M., Schuster, S. C., Suen, G., Treuner-Lange, A., Velicer, G. J., Vorhölter, F. J., Weissman, K. J., Welch, R. D., Wenzel, S. C., Whitworth, D. E., Wilhelm, S., Wittmann, C., Blocker, H., Puhler, A., and Muller, R. (2007) Complete genome sequence of the Myxobacterium *Sorangium cellulosum*. *Nat. Biotechnol.* **25,** 1281–1289
18. Huntley, S., Hamann, N., Wegener-Feldbrügge, S., Treuner-Lange, A., Kube, M., Reinhardt, R., Klages, S., Müller, R., Ronning, C. M., Nierman, W. C., and Søgaard-Andersen, L. (2011) Comparative genomic analysis of fruiting body formation in *Myxococcales*. *Mol. Biol. Evol.* **28,** 1083–1097
19. Huntley, S., Zhang, Y., Treuner-Lange, A., Kneip, S., Sensen, C. W., and Søgaard-Andersen, L. (2012) Complete genome sequence of the fruiting *Myxobacterium corallococcus* coralloides DSM 2259. *J. Bacteriol.* **194,** 3012–3013
20. Inouye, S., Nariya, H., and Munoz-Dorado, J. (2008) in *Myxobacteria: Multicellularity and Differentiation* (Whitworth, D. E., ed) pp. 191–210, American Society for Microbiology, Washington, D. C.
21. Pérez, J., Castañeda-García, A., Jenke-Kodama, H., Müller, R., and Muñoz-Dorado, J. (2008) Eukaryotic-like protein kinases in the prokaryotes and the myxobacterial kinome. *Proc. Natl. Acad. Sci. U.S.A.* **105,** 15950–15955
22. Whitworth, D. E., and Cock, P. J. (2008) Two-component systems of the myxobacteria. Structure, diversity, and evolutionary relationships. *Microbiology* **154,** 360–372
23. Whitworth, D. E., and Cock, P. J. (2008) in *Myxobacteria: Multicellularity and Differentiation* (Whitworth, D. E., ed) pp. 169–189, American Society for Microbiology, Washington, D. C.
24. Shi, X., Wegener-Feldbrügge, S., Huntley, S., Hamann, N., Hedderich, R., and Søgaard-Andersen, L. (2008) Bioinformatics and experimental analysis of proteins of two-component systems in *Myxococcus xanthus*. *J. Bacteriol.* **190,** 613–624
25. Zusman, D. R., Scott, A. E., Yang, Z., and Kirby, J. R. (2007) Chemosensory pathways, motility, and development in *Myxococcus xanthus*. *Nat. Rev. Microbiol.* **5,** 862–872
26. Lee, B., Holkenbrink, C., Treuner-Lange, A., and Higgs, P. I. (2012) *Myxococcus xanthus* developmental cell fate production: heterogeneous accumulation of developmental regulatory proteins and reexamination of the role of MazF in developmental lysis. *J. Bacteriol.* **194,** 3058–3068
27. Janssen, G. R., and Dworkin, M. (1985) Cell-cell interactions in developmental lysis of *Myxococcus xanthus*. *Dev. Biol.* **112,** 194–202
28. Nariya, H., and Inouye, M. (2008) MazF, an mRNA interferase, mediates programmed cell death during multicellular *Myxococcus* development. *Cell* **132,** 55–66
29. O'Connor, K. A., and Zusman, D. R. (1991) Behavior of peripheral rods and their role in the life cycle of *Myxococcus xanthus*. *J. Bacteriol.* **173,** 3342–3355
30. O'Connor, K. A., and Zusman, D. R. (1991) Development in *Myxococcus xanthus* involves differentiation into two cell types, peripheral rods and spores. *J. Bacteriol.* **173,** 3318–3333
31. Sun, H., and Shi, W. (2001) Genetic studies of *mrp*, a locus essential for cellular aggregation and sporulation of *Myxococcus xanthus*. *J. Bacteriol.* **183,** 4786–4795
32. Ueki, T., and Inouye, S. (2003) Identification of an activator protein required for the induction of *fruA*, a gene essential for fruiting body development in *Myxococcus xanthus*. *Proc. Natl. Acad. Sci. U.S.A.* **100,** 8782–8787
33. Nariya, H., and Inouye, S. (2005) Identification of a protein Ser/Thr kinase cascade that regulates essential transcriptional activators in *Myxococcus xanthus* development. *Mol. Microbiol.* **58,** 367–379
34. Nariya, H., and Inouye, S. (2006) A protein Ser/Thr kinase cascade negatively regulates the DNA-binding activity of MrpC, a smaller form of which may be necessary for the *Myxococcus xanthus* development. *Mol. Microbiol.* **60,** 1205–1217
35. Müller, F. D., Treuner-Lange, A., Heider, J., Huntley, S. M., and Higgs, P. I. (2010) Global transcriptome analysis of spore formation in *Myxococcus xanthus* reveals a locus necessary for cell differentiation. *BMC Genomics* **11,** 264
36. Higgs, P. I., Jagadeesan, S., Mann, P., and Zusman, D. R. (2008) EspA, an orphan hybrid histidine protein kinase, regulates the timing of expression of key developmental proteins of *Myxococcus xanthus*. *J. Bacteriol.* **190,** 4416–4426
37. Cho, K., and Zusman, D. R. (1999) Sporulation timing in *Myxococcus xanthus* is controlled by the espAB locus. *Mol. Microbiol.* **34,** 714–725
38. Rasmussen, A. A., and Søgaard-Andersen, L. (2003) TodK, a putative histidine protein kinase, regulates timing of fruiting body morphogenesis in *Myxococcus xanthus*. *J. Bacteriol.* **185,** 5452–5464
39. Lee, B., Higgs, P. I., Zusman, D. R., and Cho, K. (2005) EspC is involved in controlling the timing of development in *Myxococcus xanthus*. *J. Bacteriol.* **187,** 5029–5031
40. Cho, K., Treuner-Lange, A., O'Connor, K. A., and Zusman, D. R. (2000)

Developmental aggregation of *Myxococcus xanthus* requires *frgA*, an frz-related gene. *J. Bacteriol.* **182,** 6614–6621
41. Stein, E. A., Cho, K., Higgs, P. I., and Zusman, D. R. (2006) Two Ser/Thr protein kinases essential for efficient aggregation and spore morphogenesis in *Myxococcus xanthus*. *Mol. Microbiol.* **60,** 1414–1431
42. Lee, B., Schramm, A., Jagadeesan, S., and Higgs, P. I. (2010) Two-component systems and regulation of developmental progression in *Myxococcus xanthus*. *Methods Enzymol.* **471,** 253–278
43. Maniatis, T., Fritsch, E. F., and Sambrook, J. (1982) *Molecular Cloning: A Laboratory Manual*, Cold Spring Harbor Laboratory Press, Cold Spring Harbor, NY
44. Ueki, T., Inouye, S., and Inouye, M. (1996) Positive-negative KG cassettes for construction of multigene deletions using a single drug marker. *Gene* **183,** 153–157
45. Zheng, L., Baumann, U., and Reymond, J. L. (2004) An efficient one-step site-directed and site-saturation mutagenesis protocol. *Nucleic Acids Res.* **32,** e115
46. Li, Z. F., Li, X., Liu, H., Liu, X., Han, K., Wu, Z. H., Hu, W., Li, F. F., and Li, Y. Z. (2011) Genome sequence of the halotolerant marine bacterium *Myxococcus fulvus* HW-1. *J. Bacteriol.* **193,** 5015–5016
47. Thomas, S. H., Wagner, R. D., Arakaki, A. K., Skolnick, J., Kirby, J. R., Shimkets, L. J., Sanford, R. A., and Löffler, F. E. (2008) The mosaic genome of *Anaeromyxobacter dehalogenans* strain 2CP-C suggests an aerobic common ancestor to the δ-proteobacteria. *PLoS ONE* **3,** e2103
48. Ivanova, N., Daum, C., Lang, E., Abt, B., Kopitz, M., Saunders, E., Lapidus, A., Lucas, S., Glavina Del Rio, T., Nolan, M., Tice, H., Copeland, A., Cheng, J. F., Chen, F., Bruce, D., Goodwin, L., Pitluck, S., Mavromatis, K., Pati, A., Mikhailova, N., Chen, A., Palaniappan, K., Land, M., Hauser, L., Chang, Y. J., Jeffries, C. D., Detter, J. C., Brettin, T., Rohde, M., Göker, M., Bristow, J., Markowitz, V., Eisen, J. A., Hugenholtz, P., Kyrpides, N. C., and Klenk, H. P. (2010) Complete genome sequence of *Haliangium ochraceum* type strain (SMP-2). *Stand. Genomic Sci.* **2,** 96–106
49. Abramoff, M. D., Magalhaes, P. J., and Ram, S. J. (2004) Image processing wit ImageJ. *Biophotonics Int.* **11,** 36–42
50. Nath, K., and Koch, A. L. (1970) Protein degradation in *Escherichia coli*. I. Measurement of rapidly and slowly decaying components. *J. Biol. Chem.* **245,** 2889–2900
51. Segal, H. L., and Kim, Y. S. (1963) Glucocorticoid stimulation of the biosynthesis of glutamic-alanine transaminase. *Proc. Natl. Acad. Sci. U.S.A.* **50,** 912–918
52. Arias, I. M., Doyle, D., and Schimke, R. T. (1969) Studies on the synthesis and degradation of proteins of the endoplasmic reticulum of rat liver. *J. Biol. Chem.* **244,** 3303–3315
53. Belle, A., Tanay, A., Bitincka, L., Shamir, R., and O'Shea, E. K. (2006) Quantification of protein half-lives in the budding yeast proteome. *Proc. Natl. Acad. Sci. U.S.A.* **103,** 13004–13009
54. Hsing, W., and Silhavy, T. J. (1997) Function of conserved histidine-243 in phosphatase activity of EnvZ, the sensor for porin osmoregulation in *Escherichia coli*. *J. Bacteriol.* **179,** 3729–3735
55. Chen, Y. E., Tsokos, C. G., Biondi, E. G., Perchuk, B. S., and Laub, M. T. (2009) Dynamics of two phosphorelays controlling cell cycle progression in *Caulobacter crescentus*. *J. Bacteriol.* **191,** 7417–7429
56. Dutta, R., Yoshida, T., and Inouye, M. (2000) The critical role of the conserved Thr-247 residue in the functioning of the osmosensor EnvZ, a histidine kinase/phosphatase, in *Escherichia coli*. *J. Biol. Chem.* **275,** 38645–38653
57. Jiang, P., Atkinson, M. R., Srisawat, C., Sun, Q., and Ninfa, A. J. (2000) Functional dissection of the dimerization and enzymatic activities of *Escherichia coli* nitrogen regulator II and their regulation by the PII protein. *Biochemistry* **39,** 13433–13449
58. Wolfe, A. J. (2010) Physiologically relevant small phosphodonors link metabolism to signal transduction. *Curr. Opin. Microbiol.* **13,** 204–209
59. Paul, R., Jaeger, T., Abel, S., Wiederkehr, I., Folcher, M., Biondi, E. G., Laub, M. T., and Jenal, U. (2008) Allosteric regulation of histidine kinases by their cognate response regulator determines cell fate. *Cell* **133,** 452–461
60. Goodman, A. L., Merighi, M., Hyodo, M., Ventre, I., Filloux, A., and Lory, S. (2009) Direct interaction between sensor kinase proteins mediates acute and chronic disease phenotypes in a bacterial pathogen. *Genes Dev.* **23,** 249–259
61. Sun, H., and Shi, W. (2001) Analyses of *mrp* genes during *Myxococcus xanthus* development. *J. Bacteriol.* **183,** 6733–6739
62. Hengge, R. (2009) Proteolysis of σS (RpoS) and the general stress response in *Escherichia coli*. *Res. Microbiol.* **160,** 667–676
63. Iniesta, A. A., McGrath, P. T., Reisenauer, A., McAdams, H. H., and Shapiro, L. (2006) A phospho-signaling pathway controls the localization and activity of a protease complex critical for bacterial cell cycle progression. *Proc. Natl. Acad. Sci. U.S.A.* **103,** 10935–10940
64. Nikolskaya, A. N., Mulkidjanian, A. Y., Beech, I. B., and Galperin, M. Y. (2003) MASE1 and MASE2. Two novel integral membrane sensory domains. *J. Mol. Microbiol. Biotechnol.* **5,** 11–16
65. Henry, J. T., and Crosson, S. (2011) Ligand-binding PAS domains in a genomic, cellular, and structural context. *Annu. Rev. Microbiol.* **65,** 261–286
66. Pallen, M., Chaudhuri, R., and Khan, A. (2002) Bacterial FHA domains. Neglected players in the phosphothreonine signaling game? *Trends Microbiol.* **10,** 556–563
67. Campos, J. M., and Zusman, D. R. (1975) Regulation of development in *Myxococcus xanthus*. Effect of 3′,5′-cyclic AMP, ADP, and nutrition. *Proc. Natl. Acad. Sci. U.S.A.* **72,** 518–522
68. Julien, B., Kaiser, A. D., and Garza, A. (2000) Spatial control of cell differentiation in *Myxococcus xanthus*. *Proc. Natl. Acad. Sci. U.S.A.* **97,** 9098–9103